Published in final edited form as:
Arterioscler Thromb Vasc Biol. 2009 December ; 29(12): 2083–2089. doi:10.1161/ATVBAHA.109.193227.

Discrete contributions of elastic fiber components to arterial development and mechanical compliance

Luca Carta[1,*], **Jessica E. Wagenseil**[2,*], **Russell H. Knutsen**[3], **Boubacar Mariko**[4], **Gilles Faury**[4], **Elaine C. Davis**[5], **Barry Starcher**[6], **Robert P. Mecham**[3], and **Francesco Ramirez**[1]

[1]Department of Pharmacology and Systems Therapeutics and the Cardiovascular Institute, Mount Sinai School of Medicine, New York, NY

[2]Department o Biomedical Engineering, Saint Louis University, St. Louis, MO

[3]Department of Cell Biology and Physiology, Washington University School of Medicine, St. Louis, MO

[4]Université Joseph Fourier, Grenoble, France

[5]Department of Anatomy and Cell Biology, McGill University, Montreal, Canada

[6]University of Texas Health Science Center, Tyler, TX

Abstract

Objective—Even though elastin and fibrillin-1 are the major structural components of elastic fibers, mutations in elastin and fibrillin-1 lead to narrowing of large arteries in supravascular aortic stenosis and dilation of the ascending aorta in Marfan syndrome, respectively. A genetic approach was therefore employed here to distinguish the differential contributions of elastin and fibrillin-1 to arterial development and compliance.

Methods and Results—Key parameters of cardiovascular function were compared among adult mice haploinsufficient for elastin (*Eln*$^{+/-}$), fibrillin-1 (*Fbn1*$^{+/-}$), or both proteins (*dHet*). Physiological and morphological comparisons correlate elastin haploinsufficiency with increased blood pressure and vessel length and tortuosity in *dHet* mice, and fibrillin-1 haploinsufficiency with increased aortic diameter in the same mutant animals. Mechanical tests confirm that elastin and fibrillin-1 impart elastic recoil and tensile strength to the aortic wall, respectively. Additional *ex vivo* analyses demonstrate additive and overlapping contributions of elastin and fibrillin-1 to the material properties of vascular tissues. Lastly, light and electron microscopy evidence implicates fibrillin-1 in the hypertension-promoted remodeling of the elastin-deficient aorta.

Conclusions—These results demonstrate that elastin and fibrillin-1 have both differential and complementary roles in arterial wall formation and function, and advance our knowledge of the structural determinants of vascular physiology and disease.

Keywords

elastin; fibrillin-1; hypertension; Marfan syndrome; supravalvular aortic stenosis

Correspondence to Francesco Ramirez, Ph.D., Department Pharmacology and Systems Therapeutics, Mount Sinai School of Medicine, One Gustave L Levy Place, Box 1603, New York, NY 10029, Telephone: 212-241-7237, Fax: 212-996-7214, francesco.ramirez@mssm.edu.
*These authors contributed equally to the study

Disclosures
None.

Introduction

Elastic fibers together with smooth muscle cells (SMCs) form the lamellar units that distribute hemodynamic tension uniformly throughout the vessel wall and confer elastic recoil to large arteries.[1] Elastic fibers consist of fibrillin microfibrils surrounding and embedded within an amorphous core of elastin.[1,2] Fibrillins are large glycoproteins that polymerize into microfibrils that associate with elastin and other elastic fiber proteins.[2] Elastin is secreted as soluble tropoelastin molecules that are subsequently cross-linked by lysyl oxydase enzymes to become insoluble elastin.[1] Fibrillin-rich microfibrils are believed to provide a structural scaffold that guides elastin deposition and assembly in concert with other elastic fiber molecules.[1,2]

In spite of being part of the same extracellular macroaggregate, elastin haploinsufficiency in supravalvular aortic stenosis (SVAS, OMIM #185500) leads to narrowing of large elastic arteries, whereas mutations of fibrillin-1 in Marfan syndrome (MFS, OMIM #154700) result in aortic dilation.[1,3] Mouse models of SVAS and MFS have yielded mechanistic insights underlying the vascular phenotype of these two conditions.[4–14] Elastin haploinsufficient mice are viable and display an increased number of lamellar units due to a developmental adaptation to abnormally high blood pressure.[6,10,11,13] Mice under-expressing fibrillin-1 die from aortic rupture between 2 to 4 months of age and show no changes in blood pressure or in the number of lamellar units.[7–9] No comparable information is currently available for fibrillin-1 haploinsufficient mice.[15]

In order to characterize the contributions of elastin and fibrillin-1 to arterial function, we examined several different properties of vessels haploinsufficient for both proteins. The phenotypes of mice haploinsufficient for elastin or fibrillin-1 or both proteins suggest no major involvement of fibrillin-1 microfibrils in elastin-dependent maintenance of baseline blood pressure and vessel morphology, reiterate the discrete functions of fibrillin-1 and elastin in arterial compliance, and reveal cooperation between the two proteins in conferring material properties to arterial tissues. Additional evidence indicates that fibrillin-1 participates in the hypertension-driven process of adaptive remodeling of the aortic wall.

Methods

Animals

Seven month-old C57Bl/6J wild-type (*WT*) mice and mice haploinsufficient for elastin ($Eln^{+/-}$)[6], fibrillin-1 ($Fbn1^{+/-}$)[15], or both proteins (*dHet*) were employed in the studies following the institutional guidelines.

ECM analyses

The amounts of elastin and collagen incorporated into the arterial walls of various mutant mice were quantified using standard measurements of tissue desmosin and hydroxyproline content, respectively.[16,17] Lacking a comparable biochemical assay, relative levels of fibrillin-1 in wild-type and mutant aortae were estimated by measuring the intensity of immunoreactive material in tissues treated with increasing dilutions (from 1:100 to 1:400) of antibody pAB9543[18] with the aid of Photoshop Software (Adobe System Inc., San Jose', CA). Values were expressed using arbitrary intensity units per total tissue area (in μm^2); only values within the linear range of antibody dilution were deemed as informative.

Surgical procedures, and physiological and morphological analyses

Mice were anesthetized with 1.5% isoflurane and body temperature was maintained through a heating pad system with feedback control (Fine Science Tools, Foster City, CA). Arterial blood pressure was measured using a catheter (Millar Instruments, Houston, TX) inserted into

the right common carotid artery.[10,11] Isoflurane was reduced to 0.5% and blood pressure was monitored for 15 min while systolic, diastolic, and mean pressure were recorded. Hearts were dissected, washed, and weighed; the right ventricle was removed and the left ventricle and septum were weighed alone. Ratios of total heart weight to body weight (THW/BW) and left ventricle plus septum weight to body weight (LVW/BW) were calculated. The ascending aorta and left common carotid artery were exposed and small particles (30 to 90 μm in diameter) of activated charcoal (Sigma, St. Louis, MO) were placed on the ventral surface along the length of the carotid artery to measure *in vivo* stretch. *In vivo* stretch was not assessed for ascending aortae because it is minimal compared to carotid arteries and is not significantly different between *WT* and $Eln^{+/-}$ aortae.[11] *In vivo* images of each carotid artery were recorded with a stereomicroscope coupled to a video camera. Carotid arteries were removed, placed in physiological saline solution, and images were recorded *ex vivo* before mechanical testing. The ratio of *in vivo* to *ex vivo* lengths was calculated by measuring the distance between three sets of carbon particles evenly spaced along the carotid length using Image J software. Images of the ascending aorta were also recorded *in vivo* and *ex vivo*. The distance between the base of the heart and the innominate artery was measured *in vivo* using Image J software to determine the length of the ascending aorta.[14]

Mechanical tests

Arteries were placed on stainless steel cannulae mounted in a pressure and force arteriograph (Danish Myotechnology, Copenhagen, Denmark) and the unloaded length was recorded. Each artery was preconditioned for three cycles during which the length was adjusted to the *in vivo* length at which the force decreased slightly with pressure. The *in vivo* length was further verified by comparing the stretch of the artery (with respect to the unloaded length) to previously determined *in vivo* stretch ratios.[12] Stretch of carotid arteries during mechanical testing was similar to the *in vivo* value. The artery was then pressurized for three cycles from 0 to 175 mmHg in increments of 25 mmHg (12 sec/step) while pressure, outer diameter, and longitudinal force were recorded at 1 Hz. After mechanical testing, 2–3 rings (1–2 mm long) were cut from the center of the artery and imaged to obtain the unloaded diameter and thickness. Artery boundaries were determined manually and measured using Image J software. Pressure, diameter, longitudinal force and longitudinal stretch data were converted to stress and stretch ratios.[11] Aortic rings (1–2 mm long) were cut radially to measure the opening angle. Opening angle was not measured in carotid arteries because this parameter is unaffected by elastin haploinsufficiency.[11] The opening angle is defined as the angle subtended by the lines connecting the midpoint of the inner circumference with the ends of the ring.[19]

Light and electron microscopy

For histology, ascending aortae were fixed overnight in 4% paraformaldehyde at 4°C and processed for paraffin embedding. Sections were excised where the pulmonary artery courses behind the ascending aorta and then stained with Weigert solution.[15] Two individuals, blinded to the genotype, counted the number of elastic lamellae at four equal intervals in sections of the entire ring of the ascending aorta.[6] This approach was applied to four equally distanced rings along the vessel length of each mouse. All measurements were averaged for each aorta. For electron microscopy (EM), aortae were fixed by cardiac perfusion of 3% glutaraldehyde in 0.1M sodium cacodylate (pH 7.4) after clearing blood with normal saline. Aortae were trimmed to a 1.5 mm ring and treated en bloc with osmium tetroxide, tannic acid and uranyl acetate.[20] Following dehydration through a graded series of methanol and infiltration with Epon, tissues were embedded in pure Epon and polymerized. Sixty nm sections were counterstained with 7% methanolic uranyl acetate and lead citrate and viewed using a Tecnai 12 transmission electron microscope at 120 kV.

Statistical analysis

Four to eight mice of each genotype were examined in various experiments. Results were evaluated using Student's *t* test and are presented as mean values ± SD; p values ≤ 0.05 were chosen as statistically significant.

Results

ECM composition, anatomy and physiology of dHet arteries

The relative amounts of elastin, fibrillin-1 and collagen proteins incorporated in the *WT*, *Fbn1*$^{+/-}$, *Eln*$^{+/-}$ and *dHet* aortic walls are proportional to the number of the respective genes in each of the mutant mouse lines (Table 1). Concordance between gene expression and tissue protein levels thus excludes the formal possibility of a substantial adaptation in ECM assembly that is secondary to the mechanical changes of mutant vessels.

The aortae of adult *Fbn1*$^{+/-}$, *Eln*$^{+/-}$ and *dHet* mice are 10, 44 and 49% longer than *WT*, respectively (Table 2). Like *Eln*$^{+/-}$ mice, the carotid artery of *dHet* mice shows twisting *in vivo*, residual torsion *ex vivo*, and ~10–15% lower stretch ratio than the *Fbn1*$^{+/-}$ and *WT* artery (Figs. 1A and 1B, and Table 2). Additionally, *dHe*t and *Eln*$^{+/-}$ mice are both hypertensive (Table 2). Hypertension is associated with a significant increase of left ventricular wet weight in *dHet* compared to *WT* mice, and with an appreciable trend towards the same increase in *Eln*$^{+/-}$ mice (Table 3). These genetic data are at least consistent with the notion that elastin has a greater role than fibrillin-1 in establishing baseline blood pressure, maintaining arterial stretch and preventing residual torsion, and that fibrillin-1 plays a significantly lesser role than elastin in controlling arterial length.

Despite comparable ages and body weights, the average unloaded outer diameter of the ascending aorta is 12%–19% smaller in *Eln*$^{+/-}$ and *dHet* than in *WT* and *Fbn1*$^{+/-}$ mice, respectively (Table 2). Moreover, the average thickness of the ascending aorta is 11% lower in *Eln*$^{+/-}$ than *WT* mice, and the outer diameter and thickness of the carotid artery is 11%–19% smaller in *dHet* than in *WT* and *Fbn1*$^{+/-}$ mice, respectively (Table 2). These results suggest that fibrillin-1 haploinsufficiency has little impact on aortic adaptation to elastin haploinsufficiency, and may enhance the carotid artery phenotype in *dHet* mice.

Mechanical properties of dHet arteries

The mean outer diameter of the *Eln*$^{+/-}$ ascending aorta is smaller than *WT* at all pressures except between 50 and 100 mmHg, and the *Fbn1*$^{+/-}$ aorta is larger than *WT* at pressures between 50 and 150 mmHg (Fig. 2A). Importantly, the *dHet* aorta has a significantly smaller diameter at extreme pressures (0, 150 and 175 mmHg) and a significantly larger diameter at intermediate pressures (75 and 100 mmHg) compared to *WT* (Fig. 2A). Additionally, the average diameter of the *dHet* aorta at all pressures is more similar to *WT* than either the *Eln*$^{+/-}$ or *Fbn1*$^{+/-}$ aorta (Fig. 2A). These observations support the notion that elastin and fibrillin-1 endow the aortic wall with distinct mechanical properties, elastic recoil and tensile strength, respectively.

Whereas the mean outer diameter of the *Fbn1*$^{+/-}$ and *WT* carotid artery is comparable at all pressures, the *Eln*$^{+/-}$ value is significantly smaller than *WT* or *Fbn1*$^{+/-}$ at pressures greater than 75 or 0 mmHg, respectively (Fig. 2B). Additionally, the *dHet* artery has a substantially smaller diameter than the *Eln*$^{+/-}$ artery at extreme pressures (0 and 150 mmHg), the *WT* artery at all pressures except 50 mmHg, and the *Fbn1*$^{+/-}$ artery at all pressures (Fig. 2B). That fibrillin-1 haploinsufficiency exacerbates the *Eln*$^{+/-}$ phenotype implies partially overlapping functions of the two proteins in the carotid artery.

A comparable diameter of the *WT and* $Eln^{+/-}$ aorta at physiological pressure (solid black and grey arrows; Fig. 2A) supports the notion that increased blood pressure normalizes diameter and blood flow.[10,11] The abnormally extended diameter of the $Fbn1^{+/-}$ and *dHet* aorta at physiologic pressure (dotted black and grey arrows; Fig. 2A) suggests that fibrillin-1 imparts tensile strength at mid- to high-pressures. Because fibrillin-1 haploinsufficiency mostly impacts the ascending aorta, the mechanical role of each elastic fiber protein was evaluated by calculating the percent diameter change and the incremental elastic modulus (E_{inc}) of *WT* and mutant aortae. The percent diameter change is an inverse measure of vessel stiffness that does not account for differences in thickness. $Fbn1^{+/-}$, $Eln^{+/-}$ and *dHet* aortae display a biphasic profile with more change in diameter than *WT* at pressures below 100 mmHg, and less change in diameter at pressures above 100 mmHg (Fig. 2C). Moreover, the percent diameter change of the $Eln^{+/-}$ and $Fbn1^{+/-}$ aorta is exacerbated when the amount of both proteins is reduced (Fig. 2C). E_{inc} is the local slope of the stress-stretch ratio curve and thus, represents a measure of stiffness that accounts for differences in both unloaded diameter and thickness. When plotted against pressure, E_{inc} shows an increased stiffness of $Eln^{+/-}$ and $Fbn1^{+/-}$ aortae compared with *WT* above 125 mmHg, and greater than normal stiffness of the *dHet* aorta above 100 mmHg (Fig. 2D). These analyses demonstrate that reducing either elastin or fibrillin-1 content increases arterial stiffness at mid- to high pressures (>100 mmHg), and that reducing both proteins further increases stiffness in an additive fashion.

Material properties of dHet arteries

$Eln^{+/-}$, $Fbn1^{+/-}$ and *dHet* ascending aortae exhibit higher than normal circumferential stresses at pressures between 75 and 100 mmHg (Fig. 3A). Compared to *WT*, the circumferential stretch ratio is significantly higher in the $Fbn1^{+/-}$ aorta between 75 and 100 mmHg, in the $Eln^{+/-}$ aorta between 50 and 125 mmHg, and in the *dHet* aorta at all pressures except 0 mmHg (Fig. 3B). Whereas the stretch ratios of $Eln^{+/-}$ or $Fbn1^{+/-}$ aortae are comparable at any pressure, there are significant differences between *dHet* and both $Eln^{+/-}$ and $Fbn1^{+/-}$ aortae at pressures between 50 and 125 mmHg (Fig. 3B). At similar stretch ratios, the stress decreases in the $Eln^{+/-}$ and $Fbn1^{+/-}$ aorta and is further decreased in the *dHet* aorta (Fig. 3C). The findings that physiological stress and stretch ratio are higher than normal in $Eln^{+/-}$ and $Fbn1^{+/-}$ aortae and further increase in *dHet* aortae strongly argue for independent contributions of elastin and fibrillin-1 to the material properties of the aortic wall. Circumferential residual strain, which is expected to increase during vascular remodeling in response to hypertension, normalizes the circumferential strain gradient through the arterial wall.[21] Comparable results from opening angle measurements of *WT* and mutant aortae indicate that halving the amount of elastin or fibrillin-1 or both proteins has no impact on residual strain (Table 1).

Morphological changes in dHet aortae

The $Eln^{+/-}$ aorta exhibits more lamellar units than the *WT* or $Fbn1^{+/-}$ aorta (10.16 vs. 7.03), and a less pronounced increase (8.92) also characterizes the *dHet* aorta (Fig. 4A). These findings correlate with appreciably thinner elastic lamellae in the ascending aorta of $Eln^{+/-}$ and *dHet* compared to *WT* and $Fbn1^{+/-}$ mice (Fig. 4B). Using physiological pressures, radii and number of lamellar units, the tension per lamellar unit was calculated to be 1.0, 1.3, 1.0 and 1.1. Pa-m in the *WT*, $Fbn1^{+/-}$, $Eln^{+/-}$ and *dHet* aorta, respectively. Although within the physiological range, the $Fbn1^{+/-}$ and *dHet* values are higher than those of the *WT* and $Eln^{+/-}$ aorta. These results suggest that fibrillin-1 levels influence the developmental adaptation of the aortic wall to elastin deficiency.

Discussion

Characterization of the vascular phenotype in *dHet* mice has correlated hypertension, decreased vessel diameter, increased vessel length, and vessel tortuosity with elastin haploinsufficiency,

and fibrillin-1 deficiency with aortic dilation and significantly less, with increased vessel length. Together with estimates of mutant ECM composition, the analyses also indicate that perturbations of some material properties are mostly accounted for by reduction in the total amount of both proteins, which operate in either additive (aortic stiffness) or partially overlapping (carotid artery compliance) manners. Lastly, preliminary evidence suggests that fibrillin-1 participates in the developmental adaptation of $Eln^{+/-}$ arteries (number of elastic lamellae) to hypertension.

Combined reduction of elastin and fibrillin-1 levels leads to changes in the pressure-diameter relationship of the arterial wall, which restricts vessel expansion at extreme pressures and promotes expansion at intermediate physiological values. Reduced expansion of $Eln^{+/-}$ aortae at high pressures may reflect an increase in the relative ratio between collagen and elastin, which causes stiff collagen fibers to become the load-bearing elements at lower pressures. On the other hand, increased vessel expansion at intermediate physiological pressures in $Fbn1^{+/-}$ aortae conceivably reflects the mechanical role of microfibrils in opposing pressure-induced dilation.[1,22] Consistent with evolutionary considerations,[22] the fact that *dHet* aortae display abnormalities in both pressure ranges supports the notion that the two proteins have distinct functions in vessel compliance, with elastin providing elastic recoil and fibrillin-1 providing tensile strength. In accordance with previous work,[10,11] our data also indicate that normalization of aortic diameter and blood flow occurs at physiological pressures in *WT* or $Eln^{+/-}$ but not in $Fbn1^{+/-}$ or *dHet* aortae. This last finding strongly suggests that vascular compensation requires optimal fibrillin-1 levels.

Further analyses of our data indicate that elastin levels are critical for the mechanical behavior of both the ascending aorta and carotid artery, whereas fibrillin-1 levels mostly affect the ascending aorta. These findings are in agreement with the restricted vascular manifestations in MFS patients and mouse models of the disease, and imply spatially defined role(s) of fibrillin-1 microfibrils in the circulatory system.[2] Circumferential stress and stretch ratio of $Eln^{+/-}$ and $Fbn1^{+/-}$ aortae show similar increases at intermediate pressure values suggesting that elastin and fibrillin-1 cooperate in endowing the aortic wall with discrete material properties that influence the mechanical behavior. This conclusion is also supported by the observation that the stretch ratio of *dHet* aortae differs significantly from that of $Eln^{+/-}$ or $Fbn1^{+/-}$ in the same pressure range. A similar argument applies to the incremental stiffness of dHet aortae. Previous studies have highlighted the associations between increased arterial stiffness and decreased compliance with both systemic hypertension and left ventricular hypertrophy.[23,24] They have also shown that aortic stiffness is abnormally high in either elastin or fibrillin-1 deficiency.[9–11,25,26]

Although increased stiffness characterizes both $Eln^{+/-}$ and $Fbn1^{+/-}$ aortae, only the former mice are hypertensive probably because reduced fibrillin-1 levels do not decrease the unloaded aortic diameter thus maintaining normal blood flow. This observation supports our contention that hypertension is primarily caused by elastin deficiency, which restricts vessel size and causes hypertension in both $Eln^{+/-}$ and *dHet* mice. Association of elastin haploinsufficiency and hypertension with a greater number of lamellar units is also consistent with the notion that increased hemodynamic force induces wall remodeling to maintain a constant tension per lamellar unit.[6,10–13] Lamellar unit number is established during arterial development in coordination with blood pressure increases, SMC differentiation, and elastin accumulation.[1,27] Elastin deficiency causes perinatal hypertension leading to more lamellar units and lamellar tension normalization in $Eln^{+/-}$ mice.[10,11,14] The fact that *dHet* mice are hypertensive and have fewer lamellar units than $Eln^{+/-}$ mice indicates that a threshold level of fibrillin-1 is required to normalize the tension/lamellar unit ratio and thus aortic mechanics. This line of reasoning is consistent with our earlier report that the organization and maturation of lamellar units are grossly impaired in *Fbn1*-null mice.[15] Collectively, these findings advance

substantially our understanding of the structural determinants of vascular physiology and the pathological mechanisms that underlay disease progression in SVAS and MFS, and in age-related processes of vascular tissue degradation.

Acknowledgments

We thank Dr. Lynn Sakai for the generous gift of antibody pAB9543. We also acknowledge Maria del Solar for mouse husbandry and Karen Johnson for organizing the manuscript.

Source of funding

This study was supported by grants from the National Institutes of Health (AR049698; HL08756302, and HL74138), the Canadian Institute of Health (M0P86713), and the European Commission (ELAST-AGE, 6th PCRDT, # LSHM-CT-2005-018960). E.C.D. is a Canadian Research Chair.

References

1. Kelleher CM, McLean SE, Mecham RP. Vascular extracellular matrix and aortic development. Curr Top Dev Biol 2004;62:153–188. [PubMed: 15522742]
2. Ramirez F, Dietz HC. Extracellular microfibrils in vertebrate development and disease processes. J. Biol. Chem 2009;284:14677–14681. [PubMed: 19188363]
3. Brooke BS, Bayes-Genis A, Li DY. New insights into elastin and vascular disease. Trends Cardiovasc Med 2003;13:176–181. [PubMed: 12837579]
4. Pereira L, Andrikopoulos K, Tian J, Lee SY, Keene DR, Ono R, Reinhardt DP, Sakai LY, Biery NJ, Bunton T, Dietz HC, Ramirez F. Targeting of the gene encoding fibrillin-1 recapitulates the vascular aspect of Marfan syndrome. Nat Genet 1997;17:218–222. [PubMed: 9326947]
5. Li DY, Brooke B, Davis EC, Mecham RP, Sorensen LK, Boak BB, Eichwald E, Keating MT. Elastin is an essential determinant of arterial morphogenesis. Nature 1998;393:276–280. [PubMed: 9607766]
6. Li DY, Faury G, Taylor DG, Davis EC, Boyle WA, Mecham RP, Stenzel P, Boak B, Keating MT. Novel arterial pathology in mice and humans hemizygous for elastin. J Clin Invest 1998;102:1783–1787. [PubMed: 9819363]
7. Pereira L, Lee SY, Gayraud B, Andrikopoulos K, Shapiro SD, Bunton T, Biery NJ, Dietz HC, Sakai LY, Ramirez F. Pathogenetic sequence for aneurysm revealed in mice underexpressing fibrillin-1. Proc Natl Acad Sci U S A 1999;96:3819–3823. [PubMed: 10097121]
8. Bunton TE, Biery NJ, Myers L, Gayraud B, Ramirez F, Dietz HC. Phenotypic alteration of vascular smooth muscle cells precedes elastolysis in a mouse model of Marfan syndrome. Circ Res 2001;88:37–43. [PubMed: 11139471]
9. Marque V, Kieffer P, Gayraud B, Lartaud-Idjouadiene I, Ramirez F, Atkinson J. Aortic wall mechanics and composition in a transgenic mouse model of Marfan syndrome. Arterioscler Thromb Vasc Biol 2001;21:1184–1189. [PubMed: 11451749]
10. Faury G, Pezet M, Knutsen RH, Boyle WA, Heximer SP, McLean SE, Minkes RK, Blumer KJ, Kovacs A, Kelly DP, Li DY, Starcher B, Mecham RP. Developmental adaptation of the mouse cardiovascular system to elastin haploinsufficiency. J Clin Invest 2003;112:1419–1428. [PubMed: 14597767]
11. Wagenseil JE, Nerurkar NL, Knutsen RH, Okamoto RJ, Li DY, Mecham RP. Effects of elastin haploinsufficiency on the mechanical behavior of mouse arteries. Am J Physiol Heart Circ Physiol 2005;289:H1209–H1217. [PubMed: 15863465]
12. Pezet M, Jacob MP, Escoubet B, Gheduzzi D, Tillet E, Perret P, Huber P, Quaglino D, Vranckx R, Li DY, Starcer B, Boyle WA, Mecham RP, Faury G. Elastin haploinsufficiency induces alternative aging processes in the aorta. Rejuvenation Res 2008;11:97–112. [PubMed: 18173368]
13. Shifren A, Durmowicz AG, Knutsen RH, Faury G, Mecham RP. Elastin insufficiency predisposes to elevated pulmonary circulatory pressures through changes in elastic artery structure. J Appl Physiol 2008;105:1610–1619. [PubMed: 18772328]

14. Wagenseil JE, Ciliberto CH, Knutsen RH, Levy MA, Kovacs A, Mecham RP. Reduced vessel elasticity alters cardiovascular structure and function in newborn mice. Circ Res 2009;104:1217–1224. [PubMed: 19372465]
15. Carta L, Pereira L, Arteaga-Solis E, Lee-Arteaga SY, Lenart B, Starcher B, Merkel CA, Sukoyan M, Kerkis A, Hazeki N, Keene DR, Sakai LY, Ramirez F. Fibrillins 1 and 2 perform partially overlapping functions during aortic development. J Biol Chem 2006;281:8016–8023. [PubMed: 16407178]
16. Starcher B, Conrad M. A role for neutrophil elastase in the progression of solar elastosis. Connect Tissue Res 1995;31:133–140. [PubMed: 15612329]
17. Sims TJ, Bailey AJ. Quantitative analysis of collagen and elastin cross-links using a single-column system. J Chromatogr 1992;582:49–55. [PubMed: 1491057]
18. Charbonneau NL, Dzamba BJ, Ono RN, Keene DR, Corson GM, Reinhardt DP, Sakai LY. Fibrillins can co-assemble in fibrils, but fibrillin fibril composition displays cell-specific differences. J Biol Chem 2003;278:2740–2749. [PubMed: 12429739]
19. Chuong CJ, Fung YC. On residual stresses in arteries. J Biomech Eng 1986;108:189–192. [PubMed: 3079517]
20. Davis EC. Smooth muscle cell to elastic lamina connections in developing mouse aorta. Role in aortic medial organization. Lab Invest 1993;68:89–99. [PubMed: 8423679]
21. Liu SQ, Fung YC. Relationship between hypertension, hypertrophy, and opening angle of zero-stress state of arteries following aortic constriction. J Biomech Eng 1989;111:325–335. [PubMed: 2486372]
22. Faury G. Function-structure relationship of elastic arteries in evolution: from microfibrils to elastin and elastic fibres. Pathol Biol (Paris) 2001;49:310–325. [PubMed: 11428167]
23. Relf IR, Lo CS, Myers KA, Wahlqvist ML. Risk factors for changes in aorto-iliac arterial compliance in healthy men. Arteriosclerosis 1986;6:105–108. [PubMed: 3510614]
24. Girerd X, Laurent S, Pannier B, Asmar R, Safar M. Arterial distensibility and left ventricular hypertrophy in patients with sustained essential hypertension. Am Heart J 1991;122:1210–1214. [PubMed: 1833966]
25. Okamoto RJ, Xu H, Kouchoukos NT, Moon MR, Sundt TM 3rd. The influence of mechanical properties on wall stress and distensibility of the dilated ascending aorta. J Thorac Cardiovasc Surg 2003;126:842–850. [PubMed: 14502164]
26. Chung AW, Yang HH, Yeung KA, van Breemen C. Mechanical and pharmacological approaches to investigate the pathogenesis of Marfan syndrome in the abdominal aorta. J Vasc Res 2008;45:314–322. [PubMed: 18212506]
27. Katoh Y, Periasamy M. Growth and differentiation of smooth muscle cells during vascular development. Trends Cardiovasc Med 1996;6:100–106.

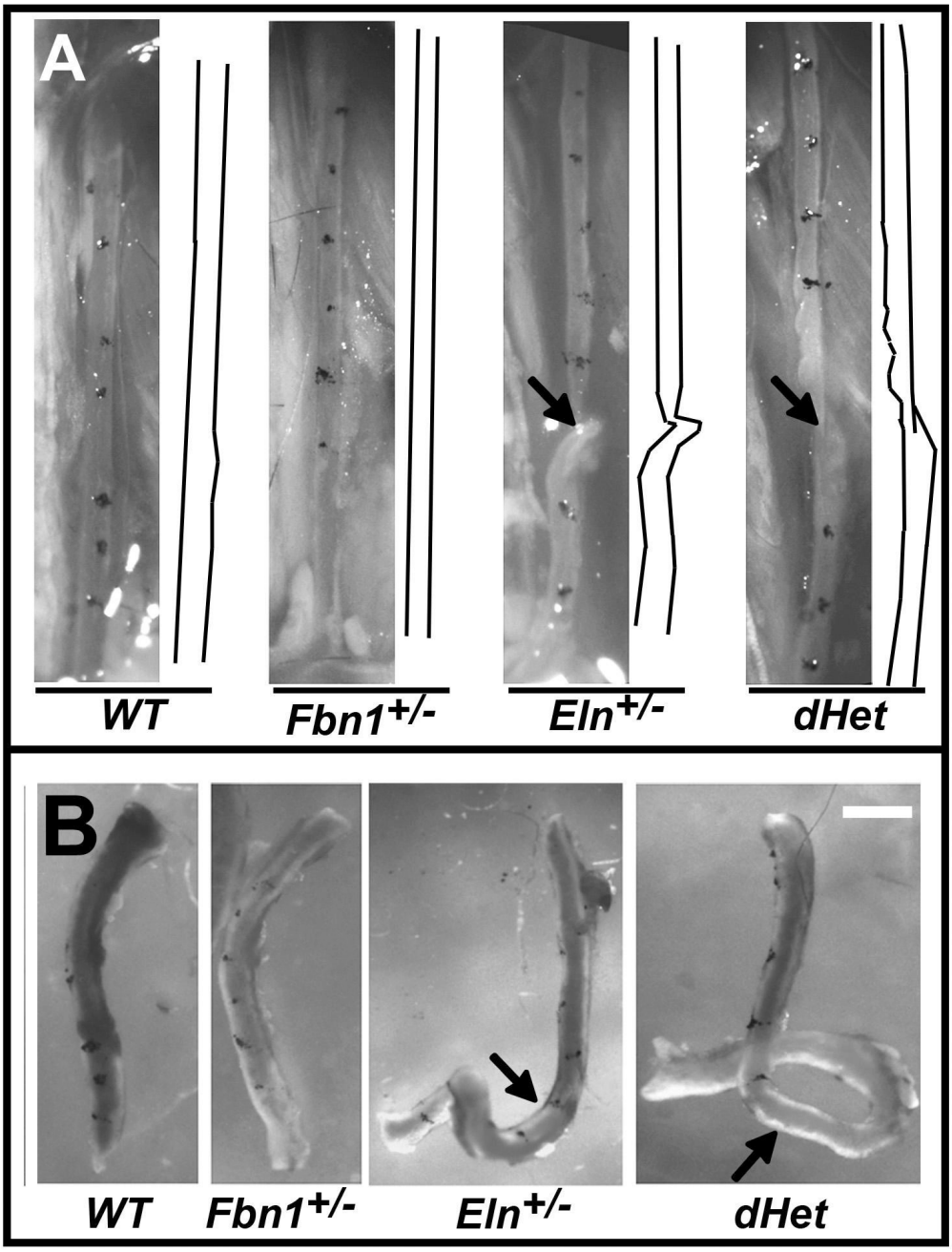

Figure 1. Morphology of ascending aortae and left common carotid arteries

*Panel **A:*** Representative left common carotid artery of *WT*, *Fbn1*$^{+/-}$, *Eln*$^{+/-}$, and *dHet* mice with the tracing of vessels shown on the right side of each image. Arrow points to a vessel twist. *Panel B*: Representative carotid arteries of the indicated genotypes upon excision with the arrows highlighting arterial tortuosity. Scale bar = 1 mm.

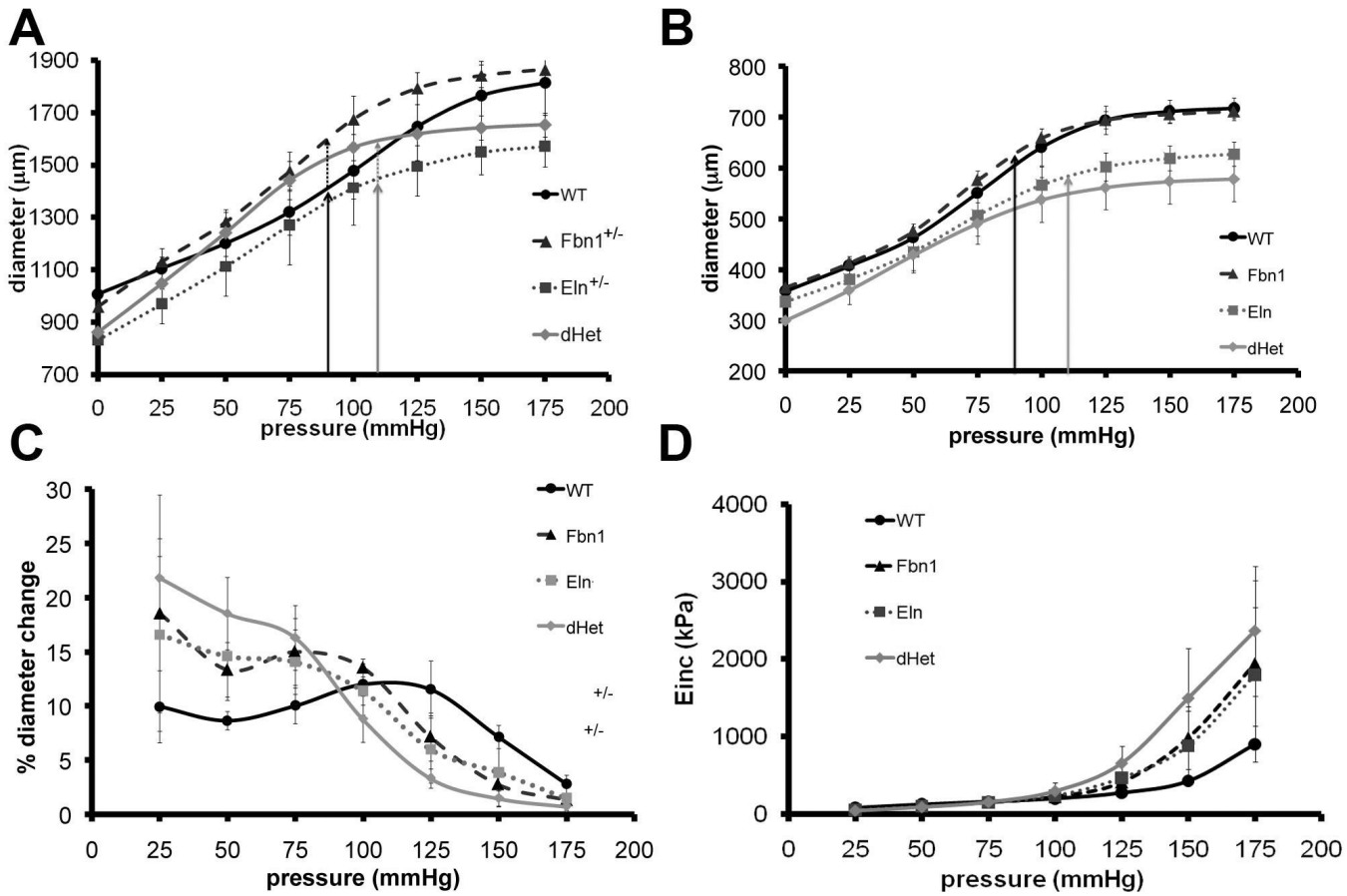

Figure 2. Mechanical testing of wild-type and mutant arteries

Panels A and B: Pressure-diameter curves of ascending aorta (*A*) and left common carotid artery (*B*) of the indicated genotypes. Vertical solid-line arrows indicate the outer diameter of *WT* (black) and *Eln*$^{+/-}$ (grey) aorta, and dotted lines indicate the outer diameter of *Fbn1*$^{+/-}$ (black) and *dHet* (grey) aorta at their respective physiological pressures. Compared with *WT* aorta, line graphs in *Panel A* show significant reduction of *Eln*$^{+/-}$ outer diameter at 0, 25, 125, 150 and 175 mmHg ($p \leq 0.05$); significant increase of *Fbn1*$^{+/-}$ outer diameter between 50 and 150 mmHg ($p \leq 0.05$); and reduced or increased outer diameter of *dHet* aorta at 0, 125, 150 and 175 mmHg, and at 75 and 100 mm Hg, respectively ($p \leq 0.05$). Line graphs also show that outer diameter of *dHet* aorta is larger than *Eln*$^{+/-}$ at pressure ≥ 50 mmHg ($p \leq 0.05$) and smaller than *Fbn1*$^{+/-}$ at 25, 75, 125, 150, and 175 mmHg ($p \leq 0.05$), whereas the outer diameter of *Eln* +/- aorta is smaller than *Fbn1*$^{+/-}$ at all pressures ($p \leq 0.05$). Line graphs in *Panel B* show significant reductions in outer diameters of *Eln*$^{+/-}$ left common carotids at 0 and 100 mmHg and above compared with *WT* ($p \leq 0.05$), and above 0 mmHg compared to *Fbn1*$^{+/-}$ ($p \leq 0.05$). Line graphs also show no differences between *Fbn1*$^{+/-}$ and *WT* carotids ($p > 0.05$), overlapping values between *dHet* and *Eln*$^{+/-}$ carotids ($p > 0.05$), smaller values than *Fbn1*$^{+/-}$ at all pressures ($p \leq 0.05$), and smaller values than *WT* at all pressures except 50 mm Hg ($p \leq 0.05$). Arteries were held at the in vivo longitudinal stretch ratio during testing. Values are means ± SD; n = 4–6 for each artery type and genotype. *Panel C:* Line graphs of the percent diameter change plotted against pressure show higher than *WT* values at 50 and 75 mmHg, and lower than *WT* values between 125 and 175 mmHg ($p \leq 0.05$) of the *Eln*$^{+/-}$ and *Fbn1*$^{+/-}$ aorta; and higher values between 25 and 75 mmHg and lower values at 100 mmHg and above ($p \leq 0.05$) of the *dHet* aorta compared to *WT*. The *dHet* aorta also has less percent diameter change than *Fbn1*$^{+/-}$ at 100 and 125 mmHg ($p \leq 0.05$). *Panel D:* Line graphs of E_{inc} plotted against pressure

show no differences between the *dHet* and $Eln^{+/-}$ aorta, and between the $Eln^{+/-}$ and $Fbn1^{+/-}$ aorta at any pressure ($p > 0.05$); lower *dHet* than *WT* values at pressures below 75mmHg and higher *dHet* than *WT* values above 100mmHg, and higher *dHet* than $Fbn1^{+/-}$ values at 125 mmHg ($p \leq 0.05$); lower $Eln^{+/-}$ than *WT* values at 50 mmHg and higher $Eln^{+/-}$ than *WT* values at 125 mmHg ($p \leq 0.05$); and higher $Fbn1^{+/-}$ than *WT* values at 125 mmHg ($p \leq 0.05$). Values are means ± SD; $n = 4–6$ for each genotype.

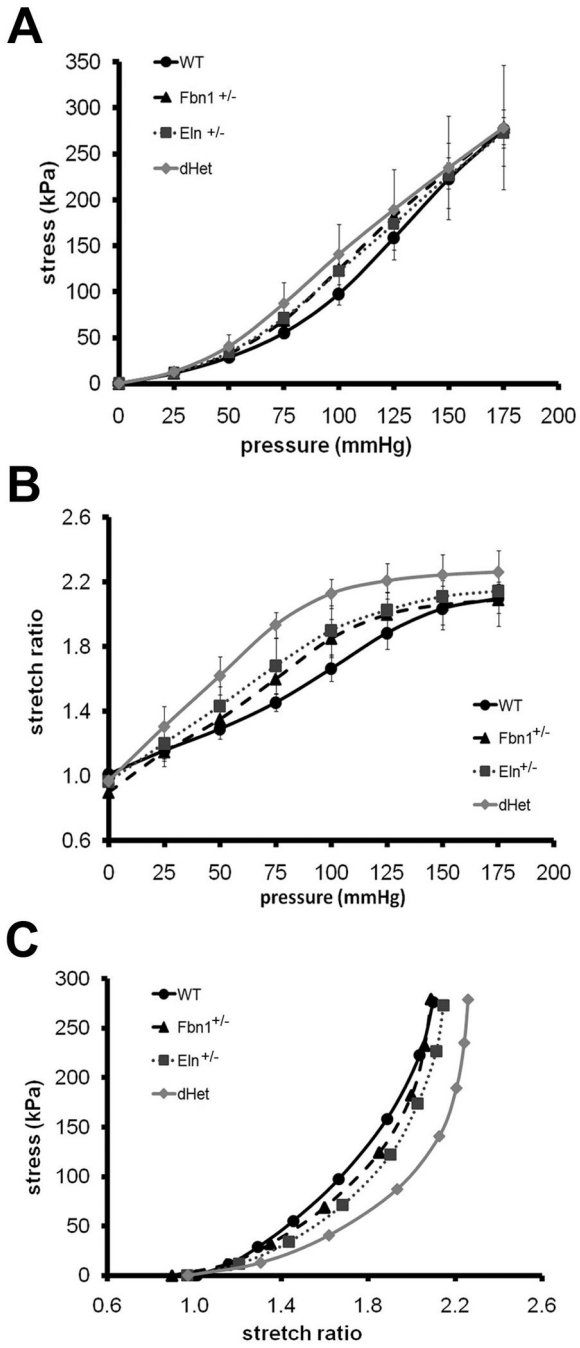

Figure 3. Circumferential stress and stretch ratio in wild-type and mutant aortae

Average circumferential stress (*Panel A*) and stretch ratio (*Panel B*) vs. pressure, and circumferential stress vs. circumferential stretch ratio (*Panel C*) in the ascending aorta of the indicated genotypes. Compared with the *WT* aorta, line graphs in *Panel A* show increased circumferential stress of the *dHet* or $Eln^{+/-}$ aorta at 75 and 100 mmHg, and of the $Fbn1^{+/-}$ aorta at 75, 100 and 125 mmHg ($p \leq 0.05$). Compared with the *WT* aorta, line graphs in *Panel B* show greater circumferential stretch ratio of the $Eln^{+/-}$ aorta at 50–125 mmHg, and of the $Fbn1^{+/-}$ aorta at 75–100 mmHg ($p \leq 0.05$). Line graphs also show that the stretch ratio of the *dHet* aorta is greater than the *WT*, $Eln^{+/-}$, or $Fbn1^{+/-}$ aorta between 25 and 175 mmHg, 50 and 125 mmHg, or 25 and 125 mmHg, respectively ($p \leq 0.05$). There are no statistical differences

between the singly haploinsufficient vessels ($p>0.05$). Line graphs in *Panel C* represent circumferential stress and stretch ratio plotted against each other for all genotypes; $Fbn1^{+/-}$ and $Eln^{+/-}$ profiles are very close to each other, $Fbn1^{+/-}$ and *WT* profiles overlap at both ends, and the *dHet* profile is appreciably shifted to the right. Values are means ± SD; $n = 4–6$ per genotype.

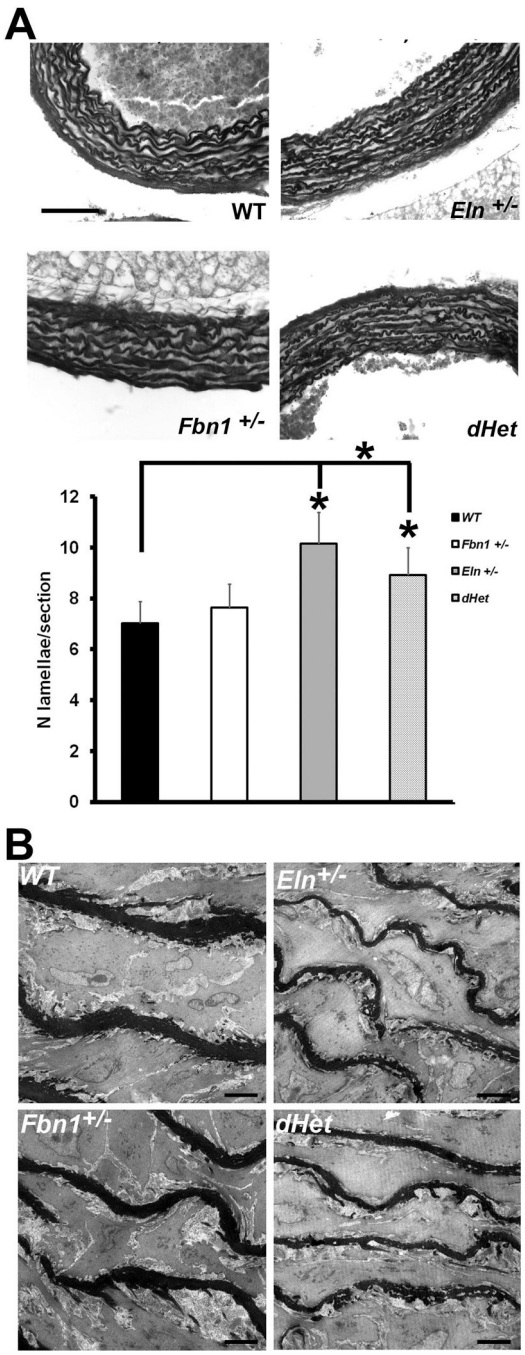

Figure 4. Aortic wall morphology

Panel A: Elastic fiber staining in the ascending aortae of the indicated genotypes. Bar graphs at the bottom summarize the average number of lamellar units in the *WT* (black), $Fbn1^{+/-}$ (white), $Eln^{+/-}$ (dark grey) or *dHet* (light grey) aorta. Asterisks indicate statistically significant differences in the number of elastic lamellae ($p \leq 0.05$). Values are means ± SD; $n = 4$ for each genotype. Scale bar = 100 μm. *Panel B*: EM images of the central medial layer of the ascending aortae in mice of the indicated genotypes. Scale bar = 5μm.

Table 1

Desmosine and hydroxyproline content (normalized to total protein) and relative intensity of immunoreactive fibrillin-1 (normalized to tissue area) in ascending aortae.

	WT	***Fbn-1*** $^{+/-}$	***Eln*** $^{+/-}$	***dHet***
Desmosine (pm/mg protein)	2976 ± 250	2769 ± 698	1385 ± 326*	1413 ± 399$^{\$}$
Hydroxyproline (μg/mg protein)	31 ± 3	34 ± 5	34 ± 6	36 ± 4
Fibrillin-1 immunoreactivity (signal intensity/ μm^2 tissue)	22.66 ± 0.83$^{€}$	9.90 ± 6.34	20.61 ± 9.61	13.99 ± 1.83
Number of mice	5	4	6	6

* $p < 0.05$ between *Eln*$^{+/-}$ and *WT or Fbn1*$^{+/-}$

$^{\$}$ $p < 0.05$ between *dHet* and *WT or Fbn1*$^{+/-}$

$^{€}$ $p < 0.05$ between *WT* and *Fbn1*$^{+/-}$ *or dHet*

Table 2

Unloaded arterial dimensions, *in vivo* stretch ratio for carotid arteries and *in vivo* length and *ex vivo* opening angle of ascending aortae.

	WT	***Fbn-1*** $^{+/-}$	***Eln*** $^{+/-}$	***dHet***
Left Common Carotid				
Thickness (μm)	94 ± 8	103 ± 12	94 ± 11	84 ± 11$^{\$}$
Outer diameter (μm)	425 ± 34	441 ± 46	400 ± 37	357 ± 32$^{\$}$
In vivo stretch ratio	1.40 ± .06	1.36 ± .05	1.23 ± .06*	1.19 ± .05$^{\$}$
Ascending Aorta				
Thickness (μm)	159 ± 13	176 ± 19	142 ± 6*	157 ± 26
Outer diameter (μm)	1017 ± 45	1066 ± 53	868 ± 45*	890 ± 51$^{\$}$
In vivo length (mm)	2.47 ± .18	2.71 ± .06$^{@}$	3.55 ± .52*	3.68 ± .19$^{\$}$
Opening angle (deg)	139 ± 36	144 ± 20	159 ± 13	160 ± 26
Tension/lamellar unit ratio (Pa-m)	1	1.3	1	1.1
Number of mice	6	4	6	6

* $p < 0.05$ between *Eln*$^{+/-}$ and *WT or Fbn1*$^{+/-}$

$^{\$}$ $p < 0.05$ between *dHet* and *WT or Fbn1*$^{+/-}$

$^{@}$ $p < 0.05$ between *Fbn1*$^{+/-}$ and *WT*

Table 3

Body weight (BW), normalized left ventricular weight (LVW/BW), normalized total heart weight (THW/BW), systolic, diastolic and mean blood pressures and heart rate of various mouse lines.

	WT	*Fbn-1* $^{+/-}$	*Eln* $^{+/-}$	*dHet*
Body weight (g)	28.96 ± 3.79	31.00 ± 2.17	34.26 ± 4.76$^{\#}$	28.96 ± 5.03
LVW/BW (mg/g)	3.02 ± 0.34	3.28 ± 0.34	3.28 ± 0.45	3.58 ± 0.43$^{\%}$
THW/BW (mg/g)	3.76 ± 0.42	4.06 ± 0.40	4.09 ± 0.57	4.41 ± 0.52
Systolic pressure (mmHg)	107 ± 4	111 ± 7	139 ± 22*	132 ± 16$^{\$}$
Diastolic pressure (mmHg)	77 ± 6	78 ± 8	91 ± 14*	85 ± 7
Mean pressure (mmHg)	91 ± 5	94 ± 7	112 ± 17*	105 ± 10$^{\%}$
Heart rate (bpm)	569 ± 59	587 ± 28	566 ± 44	562 ± 22
Number of mice	7	6	8	5

$^{\%}p < 0.05$ between *dHet* and *WT*

$^{*}p < 0.05$ between *Eln* $^{+/-}$ and *WT or Fbn1* $^{+/-}$

$^{\$}p < 0.05$ between *dHet* and *WT or Fbn1* $^{+/-}$

$^{\#}p < 0.05$ between *Fbn1* $^{+/-}$ and *WT*